ISSN: 2277-3754
ISO 9001:2008 Certified
International Journal of Engineering and Innovative Technology (IJEIT)
Volume 3, Issue 9, March 2014

Adaptive Control of Micro-grid Inverters Based on Local Parametric Optimization

Vladimir Nikulin and Viktor Ten
State University of New York, USA, Nazarbayev University, Kazakhstan

***Abstract*—This paper presents an adaptive controller for a micro-grid inverter that provides smooth interface with the main power grid. A mathematical model for the entire system is developed in the form of a transfer function. Then, a controller topology is introduced and an adaptation mechanism is developed. It is based on minimization of a performance criterion defined as a function of the error between the response of an actual system and that of a proposed reference model. This leads to excellent dynamic characteristics with a very low total harmonic distortion. The results are verified using computer simulations.**

***Index Terms*—Adaptive control, inverter, reference model, total harmonic distortion.**

I. INTRODUCTION

Control and stabilization of power systems is a very important task, especially in the days when renewable energy sources are gaining popularity. Indeed, arrays of wind turbines and photovoltaic panels are often lumped together in micro-grids that need to be properly integrated into the major power systems. This distributed power generation structure calls for localized stabilization of the voltage to make sure that each micro-grid is in compliance with the interconnect requirements, or the grid code [1]. Voltage quality and power system stability are the main requirements in most cases, and a typical assessment tool is the total harmonic distortion (THD). For both, wind farms and solar plants integrated into the power networks (120V – 69 kV) the maximum allowable THD is 5% [2, 3]. Since harmonic distortions tend to accumulate throughout the system [4], micro-grid stabilization controllers need to have acceptable harmonic rejection capabilities to facilitate seamless integration with the grid. The most promising control strategies rely on closed-loop feedback systems. Certain degree of success was reported as a result of implementation of hysteresis controllers [5]. They provide reduction of THD, but only under certain conditions, and do not perform well in case of periodic distortions caused by load nonlinearities. Several results reported in the literature are based on the internal model principle [6], which allows dealing with several harmonics at the same time. It was applied to pulse-width modulation-based (PWM) inverters [7, 8] and grid-connected inverters [9, 10]. However, some degradation of performance was observed with grid frequency variations. This issue was addressed in [11] by implementing H^{∞} repetitive voltage controller that showed noticeable improvement and offered lower complexity than its predecessor discussed in [9]. In this paper, an adaptive controller based on the reference model and local parametric optimization is proposed and tested. It is based on an adaptation law that tracks dynamics of the error and makes continuous online adjustments to the controller parameters. The algorithm has low complexity and offers good tracking performance in the presence of grid voltage perturbations.

II. SYSTEM MODEL

A. Micro-Grid Inverter

A controlled plant is a part of a system that uses renewable energy sources, such as wind energy (wind turbines) or solar energy (photovoltaic panels). It also includes a power electronics module and is connected to the grid via an LC filter and a grid interface inductor, as shown in Fig. 1.

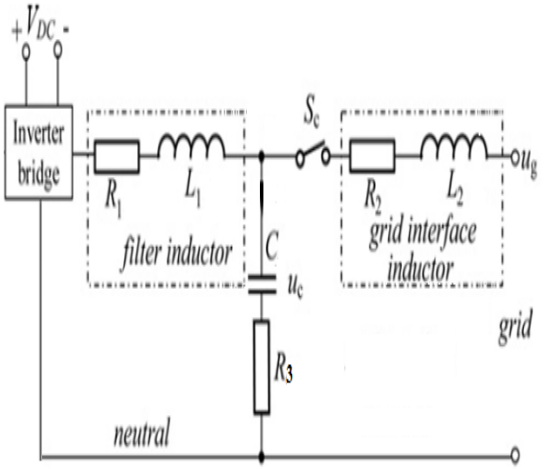

Fig 1. Micro-grid interface

The schematic includes equivalent series resistance (ESR) of the components. The switch S_c is needed for synchronization and shut-down procedures. The proposed inverter utilizes voltage-mode control [12] by sensing the output voltage and comparing it to the desired reference to correct for any signal deviations. Most inverters, including the three-phase versions, are based on H-bridge topologies, such as the circuit shown in Fig. 2.The transistors are pulse-width modulated using a PWM circuit to achieve the desired wave form shape. The following discussion leads to formulation of our modeling approach. Analogy with a different power electronics circuit that can be used to mathematically describe operation of an inverter is presented below. Consider a basic buck converter shown in Fig. 3 that can be used to represent one of the legs of a three-phase H-bridge.

ISSN: 2277-3754
ISO 9001:2008 Certified
International Journal of Engineering and Innovative Technology (IJEIT)
Volume 3, Issue 9, March 2014

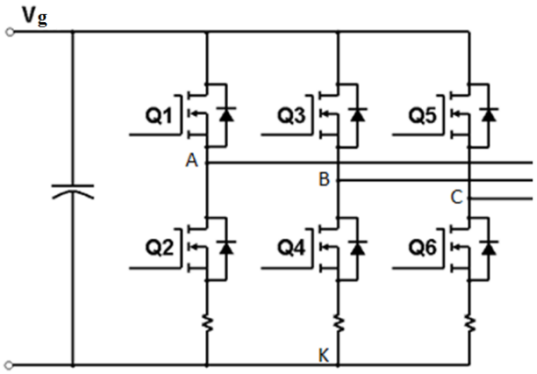

Fig 2. Three-phase H-bridge

For phase A, the active switch represents MOSFET Q1 and the passive switch is the diode connected across Q2, as shown in Fig. 2. D is the duty cycle of the active switch and D' is the duty cycle of the passive switch. The active and passive switches in any two-state PWM can be lumped in a single invariant three-terminal device called PWM switch [13].

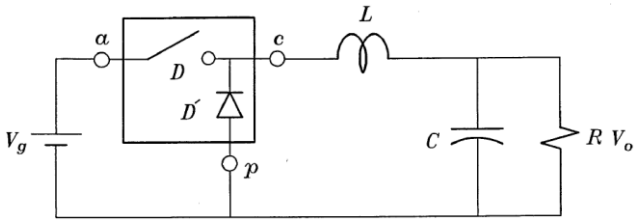

Fig 3. Three-phase H-bridge

It should be noted that buck converters are intended for generating dc output while we are trying to shape sinusoidal signals. However, considering the time scales of the switching frequency (>50 kHz) and the frequency of the ac signal (50 Hz), we can assume that over short time intervals, on the order of several switching cycles, the inverter does not change the output significantly and; therefore, can be analyzed using the above circuit. Relationships between the port voltages and currents that account for variation of the duty cycle can be expressed as

$$\begin{aligned} v_{cp}(t) &= d_s(t)\, v_{ap}(\\ i_a(t) &= d_s(t)\, i_c(t \end{aligned} \quad (1)$$

Perturbation of (1) with subsequent linearization results in the following dc and small-signal equations for terminal currents and terminal voltages, respectively

$$I_a = I_c D \hat{i}_a = I_c \hat{d} + I \quad (2)$$

$$V_{cp} = D V_{ap} \hat{v}_{cp} = V_{ap} \hat{d} + D \hat{v} \quad (3)$$

Equations (2) and (3)contain the average small-signal model of the PWM switch. The average PWM switch representation can be used to model the inverter operating in the voltage-mode control. Since the three phases of the inverter can be controlled individually and topology of the LCL filter is identical in each phase, only one phase needs to be considered. The complete dc and small-signal model of the simplified inverter phase is shown in Fig. 4. In addition to the earlier mentioned components, it includes a micro-grid load that is assumed to be purely resistive and denoted R_d.

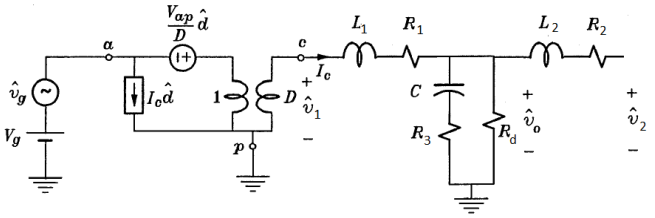

Fig 4. Equivalent model of the inverter

B. Transfer Function

Next, we can find the control-to-output transfer function by setting$\hat{v}_g = 0$ in the small-signal equivalent circuit of Fig. 4. The transfer function is generally defined in the form

$$\frac{\hat{v}_0(s)}{\hat{d}(s)} = K_D \frac{N(s)}{D(s)}, \quad (4)$$

where I is the low-frequency asymptote. The following equivalent circuit can be used in our analysis.

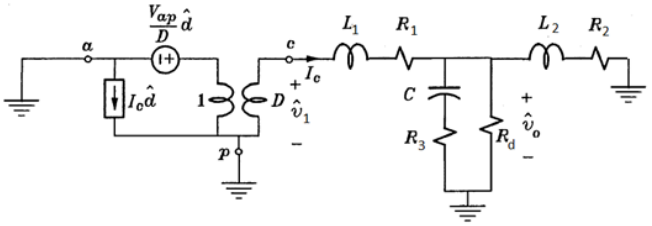

Fig 5. Control-to-output small-signal model

Inspection of Fig. 5 reveals that

$$\frac{\hat{v}_1}{D} = \frac{V_{ap}}{D} \hat{d}, \quad (5)$$

then

$$\hat{v}_1 = V_{ap} \hat{d} \quad (6)$$

It can be seen in Fig. 5 that three elements (C-R_3, R_d and L_2-R_2) appear in parallel. Their equivalent impedance can be expressed in the Laplace domain as follows:

$$Z(s) = \frac{1}{\frac{1}{R_3+\frac{1}{sC}} + \frac{1}{R_d} + \frac{1}{R_2+sL_2}} = \frac{R_d R_2 + s(R_d R_2 R_3 C + R_d L_2) + s^2 R_d R_3 L_2 C}{(R_d+R_2) + s[(R_d R_2 + R_d R_3 + R_2 R_3)C + L_2] + s^2 (R_d+R_3) I} \quad (7)$$

Then the output voltage can be found from by using the voltage divider formed by Z from (7) and a series combination L_1-R_1. First, let us find a summation of Z and L_1-R_1 as follows.

ISSN: 2277-3754
ISO 9001:2008 Certified
International Journal of Engineering and Innovative Technology (IJEIT)
Volume 3, Issue 9, March 2014

$$Z1(s) = \frac{R_dR_2+s(R_dR_2R_3C + R_dL_2) + s^2R_dR_3L_2C}{(R_d + R_2) + s[(R_dR_2 + R_dR_3+R_2R_3)C + L_2] + s^2(R_d + R_3)L_2C} + \qquad +R_1 + sL_1 =$$

$$= \frac{(R_dR_1 + R_dR_2 + R_1R_2) + s[(R_dR_1R_2+R_dR_2R_3+R_dR_1R_3+R_1R_2R_3)C + (R_d + R_2)L_1 + R_dL_2] + \frac{+s^2[(R_dR_1+R_dR_3+R_1R_3)L_2C+(R_dR_2+R_dR_3+R_2R_3)L_1C+L_1L_2]+s^3(R_d+R_3)L_1L_2C}{}}{(R_d + R_2) + s[(R_dR_2 + R_dR_3+R_2R_3)C + L_2] +} \quad (8)$$

Then, the output voltage can be found as

$$\hat{v}_o = \hat{v}_1\frac{z}{z_1} = V_{ap}\hat{d} \quad (9)$$

and the control-to-output transfer function becomes

$$\frac{\hat{v}_o(s)}{\hat{d}} = V_{ap}\frac{R_dR_2+s(R_dR_2R_3C + R_dL_2) + \frac{+s^2R_dR_3L_2C}{}}{(R_dR_1 + R_dR_2 + R_1R_2)+s[(R_dR_1R_2+R_dR_2R_3+R_dR_1R_3+R_1R_2R_3)C + (R_d + R_2)L_1 + R_dL_2] + \frac{}{+s^2[(R_dR_1+R_dR_3+R_1R_3)L_2C+(R_dR_2+R_dR_3+R_2R_3)L_1C+L_1L_2]+s^3(R_d+R_3)L_1L_2C}} \quad (11)$$

III. ADAPTIVE CONTROL SYSTEM

A. Adaptation Approach

Adaptive topology is proposed for the system discussed in the previous section. The approach relies on automatic changes of the controller characteristics to maintain the necessary performance in spite of incomplete original knowledge of the controlled process [14]. A particular branch of adaptive theory used in our system is model reference control with parametric adaptation. The model reference scheme is a mechanism that "forces" the output of an adjustable system to follow the output of the reference model. The basic assumptions are: the reference model is time-invariant linear system, the reference model and adjustable system are of the same order, and parameters of the adjustable system are accessible for adaptation. Local parametric optimization is proposed as the core design technique. The idea of the approach is to define a performance index (criterion) dependent on the adjustable parameters and to minimize this index with respect to adjustable parameters using a particular optimization method. Let the reference model [15] be given by the transfer function

$$G_m(s) = \frac{y_m(s)}{x_m(s)} = \frac{b_m^M s^m + b_{m-1}^M s^{m-1} + \cdots + b_0^M}{s^n + a_{n-1}^M s^{n-1} + \cdots + a_0^M} \quad (12)$$

Consider the adjustable system that includes the controlled plant and the adaptive controller described as follows

$$G_{as}(s) = \frac{y_{as}(s)}{x_{as}(s)} = \frac{\beta_m s^m + \beta_{m-1} s^{m-1} + \cdots + \beta_0}{s^n + \alpha_{n-1} s^{n-1} + \cdots + \alpha_0} \quad (13)$$

Then the error is found from

$$\varepsilon(t) = y_m(t) - y_{as}(t) \quad (14)$$

$$\frac{\bar{v}_o(s)}{\hat{d}} = V_{ap} \quad (10)$$

By substituting Eq. (7) and (8) into (10) and performing some simplifications we obtain

Let us define the performance index in the form below

$$J(\varepsilon, t) = \int_{t-T}^{t} \varepsilon^2(t)\, dt \quad (15)$$

Then our control strategy goal is

$$J(\varepsilon, t) = J(\alpha_i, \beta_i, t) \longrightarrow Min \quad (16)$$

that can be achieved using the gradient procedure, as follows

$$\Delta\alpha_i(t) = -\frac{k_i^a \partial J(\varepsilon,t)}{\partial \alpha_i}, i = 1,2,3, \dots, n \quad (17)$$

$$\Delta\beta_i(t) = -\frac{k_i^b \partial J(\varepsilon,t)}{\partial \beta_i}, i = 1,2,3, \dots, m \quad (18)$$

Then by using the definition of J given by (15) we can find the following derivatives of increments

$$\alpha'_i = -2k_i^a \varepsilon(t)\frac{\partial \varepsilon}{\partial \alpha_i}, i = 1,2,3, \dots, n \quad (19)$$

$$\beta'_i = -2k_i^b \varepsilon(t)\frac{\partial \varepsilon}{\partial \beta_i}, i = 1,2,3, \dots, m \quad (20)$$

In addition, partial derivatives of the errors are obtained (19) – (20)as follows

$$\frac{\partial \varepsilon(t)}{\partial \alpha_i} = \frac{\partial}{\partial \alpha_i}(y_m - y_{as}) = -\frac{\partial y_{as}}{\partial \alpha_i} \quad (21)$$

$$\frac{\partial \varepsilon(t)}{\partial \beta_i} = \frac{\partial}{\partial \beta_i}(y_m - y_{as}) = -\frac{\partial y_{as}}{\partial \beta_i} \quad (22)$$

By omitting a factor of 2, we derive the following expressions for time derivatives

$$\alpha'_i = k_i^a \varepsilon(t)\frac{\partial y_{as}}{\partial \alpha_i}, i = 1,2,3, \dots, n \quad (23)$$

$$\beta'_i = k_i^b \varepsilon(t)\frac{\partial y_{as}}{\partial \beta_i}, i = 1,2,3, \dots, m \quad (24)$$

ISSN: 2277-3754
ISO 9001:2008 Certified
International Journal of Engineering and Innovative Technology (IJEIT)
Volume 3, Issue 9, March 2014

where $k_i^a = const > 0$ and $k_i^b = const > 0$.

Derivatives $\partial y_{as}/\partial \alpha_i$ and $\partial y_{as}/\partial \beta_i$ are sensitivity functions that can be defined in a practical form. Let us re-write (13) as follows

$$y_{as}(s) = -[\sum_{i=1}^{n} \alpha_i^M(\varepsilon,t)s^i]y_{as}(s) + [\sum_{i=1}^{m} \beta_i^M(\varepsilon,t)s^i]x_{as}(s) \quad (25)$$

As an example, we can differentiate (25) with respect to adjustable parameterα_2:

$$\frac{\partial y_{as}}{\partial \alpha_2} = -s^2 y_{as} - \frac{\partial y_{as}}{\partial \alpha_2}[\sum_{i=1}^{n} \alpha_i^M(\varepsilon,t)s^i] \quad (26)$$

It is a practical assumption that parameters α_i change slowly in time, compared to the change of the control efforts [16], i.e. their time derivatives $s^i\alpha_i$ are small, then

$$\frac{\partial y_{as}}{\partial \alpha_2} = -s^2 y_{as}, \quad (27)$$

Then, sensitivity functions in (21) and (22) can be approximated as

$$\frac{\partial y_{as}}{\partial \alpha_i} = -s^i y_{as} \quad (28)$$

Similarly, by differentiating (25) with respect toβ_3 we have

$$\frac{\partial y_{as}}{\partial \beta_3} = -s^3 x_{as} - \frac{\partial y_{as}}{\partial \beta_3}[\sum_{i=1}^{n} \beta_i^M(\varepsilon,t)s^i] \quad (29)$$

Assuming that parameters β_i change slowly in time, i.e. their time derivatives $s^i\beta_i$ are small, (29) simplifies to

$$\frac{\partial y_{as}}{\partial \beta_3} = -s^3 x_{as} \quad (30)$$

Then the general form of these sensitivity functions is

$$\frac{\partial y_{as}}{\partial \beta_i} = -s^i x_{as} \quad (31)$$

Finally, the adaptation law can be formulated from (23) and (24)in the differential form

$$\alpha'_i = -k_i^a \varepsilon(t)\, s^i y_{as}, i = 1,2,3,\dots,n \quad (32)$$
$$\beta'_i = -k_i^b \varepsilon(t)\, s^i x_{as}, i = 1,2,3,\dots,m \quad (33)$$

or re-written in the integral form

$$\alpha_i = -k_i^a \int_0^t \varepsilon(t)\, s^i y_{as} dt + \alpha_i(0) \quad (34)$$
$$\beta_i = -k_i^b \int_0^t \varepsilon(t)\, s^i x_{as} dt + \beta_i(0) \quad (35)$$

This approach is known as the MIT rule. A block diagram of a system utilizing this approach is shown in Fig. 32.

B. Control Synthesis

Our controlled plant is a micro-grid inverter operating in the voltage-mode control. Its control-to-output transfer function was derived earlier and is given by Eq. (11). It is a third-order system that can be expressed as follows

$$\frac{\hat{v}_o(s)}{\hat{d}} = \frac{N_p}{D_p} = \frac{b_2 s^2 + b_1 s + b_0}{s^3 + a_2 s^2 + a_1 s + a_0} \quad (36)$$

Before obtaining the transfer function of the adjustable system we need to select desired controller configuration. In order to minimize the tracking error in the control loop, some form of an integrator can be introduced [17, 18]. The following form of a controller is proposed.

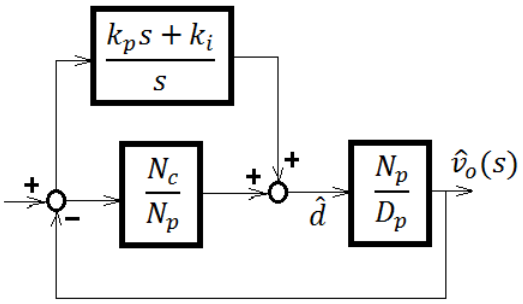

Fig 6. Proposed controller configuration

In addition to the blocks shown in Fig. 6, another controller can be introduced on the input of the system to adjust the dc gain. It should be noted that the entire feedback is composed of two parts. One is a standard proportional-integral (PI) controller with constant coefficients k_i and k_p. The other block is an adjustable controller N_c/N_p whose denominator is used to cancel the plant's zeros and the numerator has adjustable coefficients. Consider the two controllers in the plant's feedback. Let the parallel combination of the PI controller and the adaptive controller be expressed as follows.

$$\frac{N_f}{D_f} = \frac{k_p s + k_i}{s} + \frac{\hat{a}_2 s^2 + \hat{a}_1 s + \hat{a}_0}{b_2 s^2 + b_1 s + b_0} = \frac{s^3 b_2 k_p + s^2(b_2 k_i + b_1 k_p) + s(b_1 k_i + b_0 k_p) + b_0 k_i + \hat{a}_2 s^2 + \hat{a}_1 s + \hat{a}_0}{s(b_2 s^2 + b_1 s + b_0)} = \frac{s^3 b_2 k_p + s^2(b_2 k_i + b_1 k_p + \hat{a}_2) + s(b_1 k_i + b_0 k_p + \hat{a}_1) + (b_0 k_i + \hat{a}_0)}{s(b_2 s^2 + b_1 s + b_0)} \quad (37)$$

Then the overall closed-loop transfer function for the system shown in Fig. 6 can be found using (37) as follows.

$$G_{cl}(s) = \frac{\frac{N_f N_p}{D_f D_p}}{1 + \frac{N_f N_p}{D_f D_p}} \quad (38)$$

Substitution of all relevant polynomials into (38) results in

$$G_{cl}(s) = \frac{s^3 b_2 k_p + s^2(b_2 k_i + b_1 k_p + \hat{a}_2) +}{s^3(b_2 k_p + b_2) + s^2(b_2 k_i + b_1 k_p + \hat{a}_2 + b_1) +} \dots$$

ISSN: 2277-3754
ISO 9001:2008 Certified
International Journal of Engineering and Innovative Technology (IJEIT)
Volume 3, Issue 9, March 2014

$$\cdots \frac{+s(b_1 k_i + b_0 k_p + \hat{a}_1) + (b_0 k_i + \hat{a}_0)}{+s(b_1 k_i + b_0 k_p + \hat{a}_1 + b_0) + (b_0 k_i + \hat{a}_0)} \quad (39)$$

The form of equation (39) fits the previously discussed adjustable system given by Eq. (13); therefore, local parametric optimization approach can be used as previously discussed.

IV. SIMULATION RESULTS

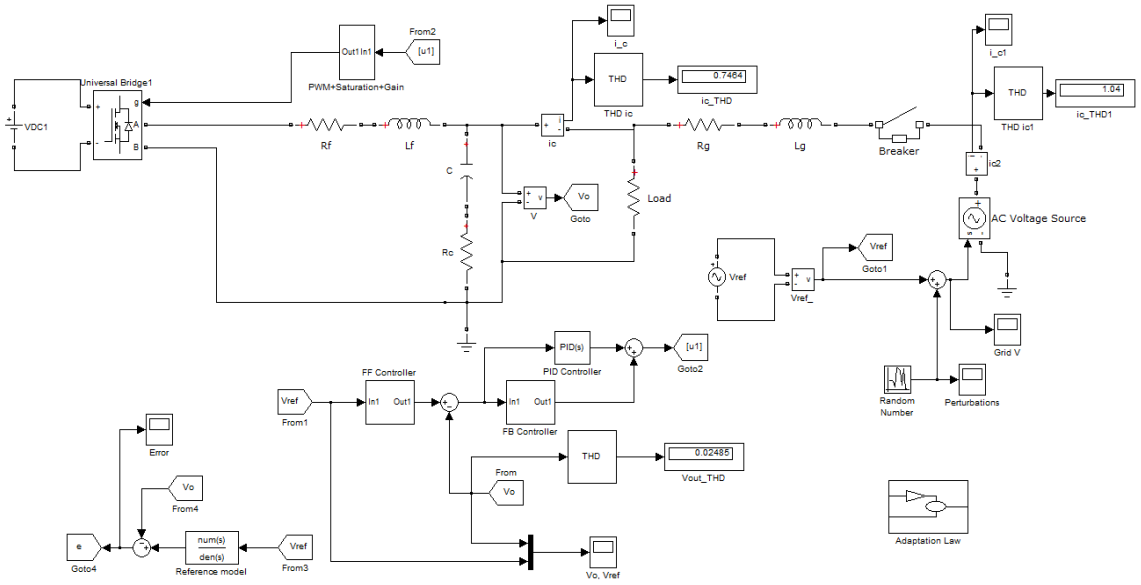

Fig 7. Simulink model of the grid-connected inverter control system

The controlled plant includes a renewable energy source, such as an array of wind turbines or photovoltaic panels. They are not shown explicitly, but their presence is indicated by a dc source VDC1, whose nominal voltage is assumed to be 50V. Only one phase of a three-phase system is presented in Fig. 7. The main utility grid is modeled by a48V-peak, 50-Hz sinusoidal voltage source. It is also assumed that grid voltage perturbations occur on a relatively slow time scale (every 5 ms) and the values of these distortions are limited by ±20% of the reference voltage Vref. Fig. 8 shows perturbations obtained from a random number generator and the resultant grid voltage with distortions is presented in Fig. 9.

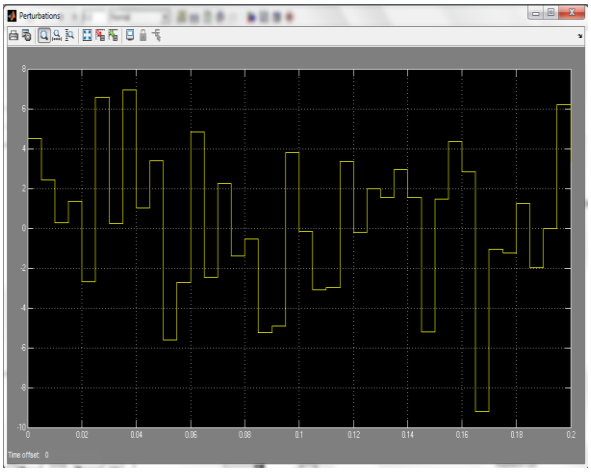

Fig 8. Perturbation signal

Voltage V_o is considered to be the output of our controlled plant. Nominal load is purely resistive with $R_d = 5\Omega$.

Nominal values of the components of the LC filter and the grid interface inductor are selected as follows:

R1 (Rf) = 0.045 Ω,
R2 (Rg) = 0.135 Ω,
R3 (Rc) = 1 Ω,
L1 (Lf) = 150 µH,
L2 (Lg) = 450 µH,
C = 22 µF.

Main power electronics components also include a pulse-width modulator (PWM) driven by a gain block with saturation, as shown in Fig. 7.

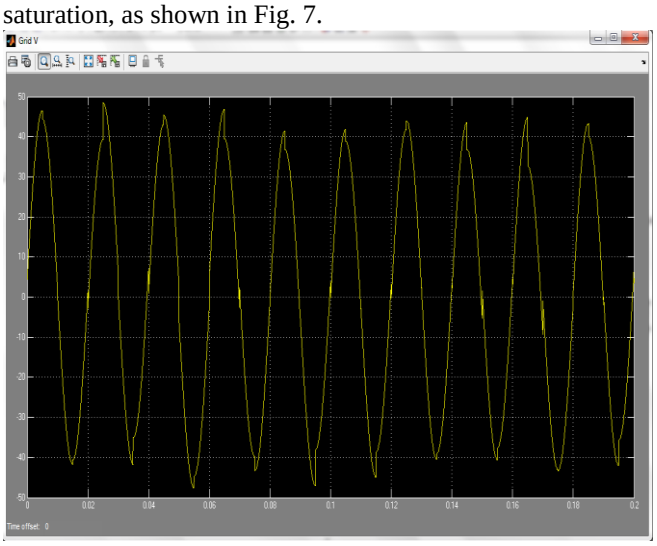

Fig 9. Grid voltage fluctuations

The adjustable feedback controller (FB controller)$N_c/N_p$is configured as discussed earlier. The denominator is a second-order polynomial and it is calculated based on the estimated values of our circuit parameters, for the

ISSN: 2277-3754
ISO 9001:2008 Certified
International Journal of Engineering and Innovative Technology (IJEIT)
Volume 3, Issue 9, March 2014

control-to-output transfer function given by (11). While the estimated polynomial may not be very precise and not cancel control plant's zeros, the discrepancy does not result in noticeable performance degradation, most likely due to the adaptation mechanism. The denominator of the FB controller has three adjustable coefficients α_0 - α_2, and their values are found as given by equation (34). A feed forward controller has only one adjustable gain β_0. It is used to tune the dc gain of the closed-loop transfer function of the adjustable system. Finally, an adaptation mechanism based on local parametric optimization (MIT rule) is used to adjust the coefficients of both controllers. The reference model was calculated by performing the pole placement procedure for a 3rd-order transfer function with poles at 10000, 15000, and 16000 rad/s. This results in the following characteristic polynomial

$$D_m = s^3 + 41000\,s^2 + 5.5e8s + 2.4e12 \quad (40)$$

Initially, the switch connecting the grid to the micro-grid is kept open. After the initial transient settles, the switch is closed, thus connecting all the system components together. Grid current drawn from the inverter is shown in Fig. 10. The current remains at zero until a breaker in the system closes at t=0.1s.

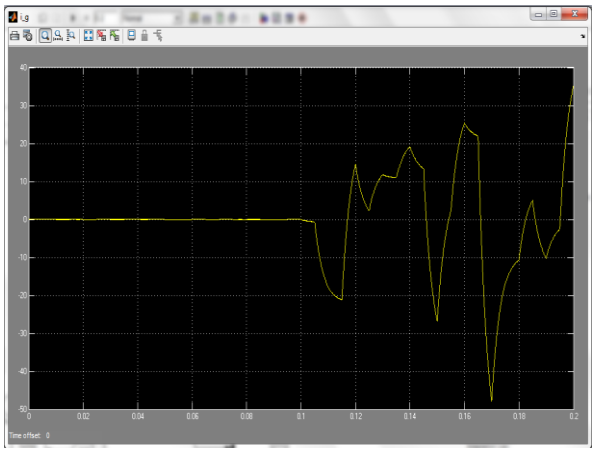

Fig 10. Grid current

Response to the commutation can also be observed by looking at the inverter current. Fig. 11 shows that the latter is fairly periodic and becomes irregular when grid perturbations reach the inverter filter.

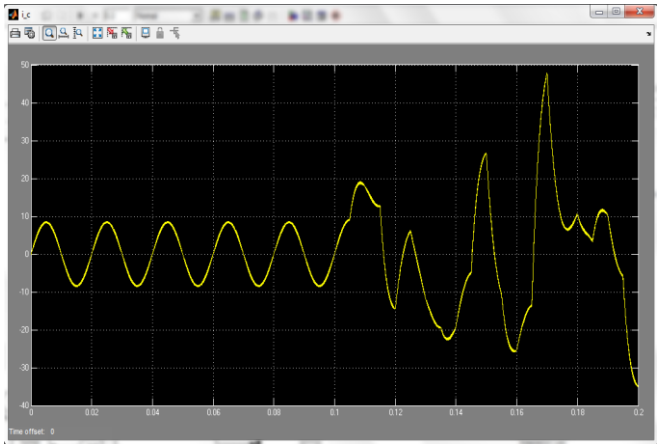

Fig 11. Inverter current

Finally, we can assess the quality of the output voltage signal. Fig. 12 features the output and reference voltages superposed together. The results indicate close fit between the actual and the desired signals.

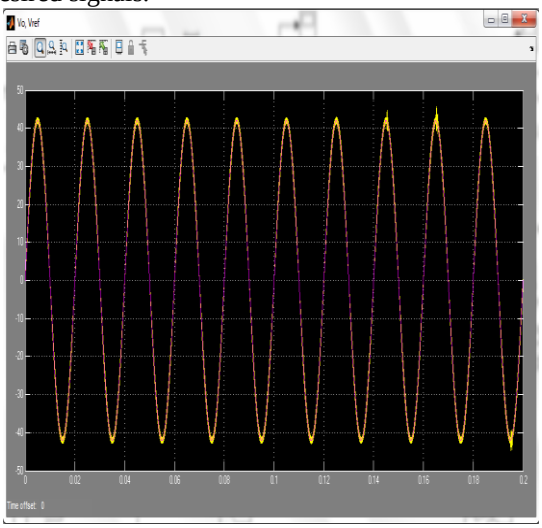

Fig 12. Reference and output voltage

The value of THD measured in the above experiment was less than 2.5%. Similar experiments reported in [11] achieved THD values closer to 3% using a more sophisticated control algorithm.

V. CONCLUSION

An adaptive control approach for micro-grid inverters was presentedin this paper. Several tasks of the system design were performed. First, a mathematical model that includes inverter power components, PWM switch, filters, and the load was developed. Then, a control system was synthesize designing adaptive algorithm that implements a local parametric optimization routine. Both the model and controller were implemented in Matlab/Simulink environment and were used as a simulation test bed for evaluating the proposed system. The results demonstrate that our design offers good performance characteristics in terms of waveform quality and the THD. While the design process included complex derivations, implementation of the final system is relatively simple. Yet, it offers all the advantages of adaptive control, including tolerance to system uncertainty, parameter variations in the controlled plant, and external disturbances.

REFERENCES

[1] Y.K. Lo and C.L. Chen, "A Voltage-Mode Controlled High-Input-Power-Factor AC Line Conditioner with Minimized Output Voltage Harmonics," Proc. PECS'94, pp. 369-374, 20-25 Jun. 1994.

[2] IEEE STANDARD,"IEEE recommended practices and requirements for harmonic control in electrical power systems." IEEE Std 519-1992, April 1993.

[3] T.M. Blooming, D.J. Carnovale, "Harmonic convergence," IEEE Ind. Appl. Mag., 2007, 13, (1), pp. 21–27.

[4] J. D. Irwin, The industrial electronics handbook (CRC Press, 1996, 2nd ed.).

ISSN: 2277-3754
ISO 9001:2008 Certified
International Journal of Engineering and Innovative Technology (IJEIT)
Volume 3, Issue 9, March 2014

[5] F. Blaabjerg, R. Teodorescu, M. Liserre, A. Timbus, "Overview of control and grid synchronization for distributed power generation systems," IEEE Trans. Ind. Electron., 2006, 53, (5), pp. 1398–1409

[6] S. Hara, Y. Yamamoto, T. Omata, M. Nakano, "Repetitive control system: a new type servo system for periodic exogenous signals," IEEE Trans. Autom. Control, 1988, 33, (7), pp. 659–668.

[7] Y. Ye, B. Zhang, K. Zhou, D. Wang, Y. Wang, "High-performance repetitive control of PWM DC-AC converters with real-time phase lead FIR filter," IEEE Trans. Circuits Syst., 2006, 53, (8), pp. 768–772.

[8] S. Chen, Y. Lai, S.-C. Tan, C. Tse, "Analysis and design of repetitive controller for harmonic elimination in PWM voltage source inverter systems," IET Power Electron., 2008, 1, (4), pp. 497–506.

[9] G. Weiss, Q. Zhong, T. Green, J. Liang, "H1 repetitive control of DC-AC converters in micro grids," IEEE Trans.Power Electron., 2004, 19, (1), pp. 219–230.

[10] Q. Zhong, T. Green, J. Liang, G. Weiss, "Robust repetitive control of grid-connected dc-ac converters," 41st IEEE Conf. on Decision and Control, Las Vegas, NV, 10–13 December 2002, vol. 3, pp. 2468–2473.

[11] T. Hornik, Q.-C. Zhong, "H∞ repetitive voltage control of grid connected inverters with a frequency adaptive mechanism," Power Electronics, IET, vol. 3, issue 6, pp. 925-935, Nov 2010.

[12] C.W. Deisch, "Switching Control Method Changes Power Converters into a Current Source," Proc. IEEE Power Electronics Specialist Conference, 1978, pp. 300-306.

[13] A.S. Kislovski, "Introduction to Dynamical Analysis of Switching dc-dc Converters," EMV Engineering, Loechliweg 47, 3000 Berne, Switzerland, 1985.

[14] S. E. Lyshevski, "Control Systems Theory with Engineering Applications,"Birkhauser, 2001.

[15] J. J. D'Azzo, C. H. Houpis, "Linear Control System Analysis and Design," McGraw-Hill, 1981.

[16] N. E. Wu, V. Nikulin, F. Heimes, and V. Skormin, "A Decentralized Approach to Fault Tolerant Flight Control," Proc. 4th IFAC Symposium on Safe process, Budapest, Hungary, 14-16 June, 2000.

[17] V. Nikulin, J. Sofka, and V. Skormin, "Advanced Lyapunov Control of a Novel Laser Beam Tracking System," Optical Engineering, Vol. 44, No. 5, May 2005, pp. 56004-1-8.

[18] V. Nikulin, R. Khandekar and J. Sofka, "Agile acousto-optic tracking system for free-space optical communications," Optical Engineering, Vol. 47, No. 6, June 2008, 064301.

AUHTOR'S PROFILE

Vladimir Nikulin received his B.S. degree in Electrical Engineering in 1996 from Karaganda Polytechnic Institute, and his M.S. and Ph.D. both in Electrical Engineering in 1998 and 2002, respectively, from the State University of New York (SUNY) at Binghamton. In 2002, he joined the Department of Electrical and Computer Engineering at SUNY-Binghamton where he is currently an Associate Professor. In 2006, he was a visiting scholar in the Department of Cybernetics at the Czech Technical University in Prague and also worked as a visiting research faculty at the U.S. Air Force Research Laboratory since 2006. His research interests include optical communications, electro-optics, advanced controls, power systems, system optimization, mathematical modeling and computer simulations.

Viktor Ten received B.S. and M.S. degrees in Electrical and Computer Engineering from Kazakh National Technical University in 2001 and Ph.D. degree in Control System Engineering from Eurasian National University, Astana, Kazakhstan in 2009.From 2001 to 2011, he was a faculty member in the Department of System Analysis and Controls, Eurasian National University, Astana. In 2008-2009 academic year, he was a Fulbright scholar in the Center for Applied Mathematics, Cornell University. Since 2011 he works as senior research scientist in Nazarbayev University Research and Innovation System. His research interests include control systems, smart grids and renewable power sources.